

## Subcritical crack propagation in rocks: theory, experimental results and applications

BARRY KEAN ATKINSON

Department of Geology, Imperial College of Science and Technology  
South Kensington, London SW7 2BP, England

(Received 29 November 1980; accepted in revised form 23 July 1981)

**Abstract**—The micromechanisms of tensile fracture are reviewed, with particular emphasis on the influence of chemical effects on fracture controlled by pre-existing cracks (stress corrosion). A fracture mechanism map for quartz is presented which was constructed using a combination of theoretical insights and experimental data. The manner in which stress corrosion will modify the predictions of fracture mechanism maps is discussed by reviewing the numerous theories of stress corrosion. Experimental data are presented on stress corrosion in tensile deformation of quartz, quartz rocks, calcite rocks, basaltic rocks, granitic rocks and other geological materials. Although the experimental evidence for stress corrosion is overwhelming, very few data were obtained under conditions that simulate those in the bulk of the earth's crust and so the extent of its geophysical significance is yet to be fully established. Examples are given, however, of how invoking stress corrosion as a rate-controlling deformation mechanism sheds new light on extremely diverse geophysical phenomena, such as: predicting the strength and sliding friction properties of rocks, modelling earthquake rupture, the stability of hot, dry-rock geothermal reservoirs, stimulation of oil and gas reservoirs, the crack-seal mechanism of rock deformation and low stress dilatancy, fracture mechanics of lunar rocks, magmatic intrusions and the relaxation of internal stresses in rock.

### INTRODUCTION

THE FRACTURE mechanics description of crack propagation (Irwin 1958) allocates a key role to the stress intensity factor,  $K$ , which is a measure of a body's resistance to fracture. Fracture propagation problems can be analysed in terms of the three stress intensity factors,  $K_I$ ,  $K_{II}$  and  $K_{III}$ , which pertain to the three fundamental modes of crack propagation. These are: mode I, tensile; mode II, in-plane shear and mode III, anti-plane shear. For a two-dimensional plane crack of any mode the stress intensity factor is given by

$$K = Y\sigma_a a^{1/2} \quad (1)$$

where  $Y$  is a geometrical constant,  $\sigma_a$  is the remote applied stress and  $a$  is a characteristic crack length.

If the stress intensity factor is raised above a critical value,  $K_c$ , which is a material constant, then the crack will propagate at velocities approaching those of sound in the medium. For many materials such as oxides and silicates, however, crack propagation can occur at much lower values of  $K$  than  $K_c$ . A variety of environmentally dependent mechanisms, notably stress corrosion, can facilitate this stable, quasistatic subcritical crack propagation. It occurs at velocities which decrease as  $K$  is lowered to some threshold value,  $K_c$ , below which no crack propagation is observed.

In recent years there has been a rapid increase in the number of experimental studies designed to advance our understanding of subcritical crack propagation in rocks. The impetus for this has come from both the extensive work of materials scientists, who have analysed

the premature failure of structural engineering components in terms of subcritical crack propagation, and the growing awareness amongst earth scientists that subcritical crack growth can explain many previously puzzling problems in geophysics.

This paper has four main sections. In the first I will outline the complexities of subcritical failure in rocks and present a fracture mechanism map for quartz to illustrate some of these phenomena. In the second section the current state of modelling some aspects of subcritical failure at a theoretical level is reviewed. The third section presents the findings of experimental studies of subcritical crack propagation in rocks. The emphasis here is on results, as experimental methods are to be reviewed elsewhere (Atkinson in preparation). The fourth section contains a number of illustrations of the potential importance of subcritical cracking in geophysical phenomena.

To a very large extent this work concentrates on results for mode I, tensile crack propagation under the influence of stress corrosion. This arises mainly because the vast majority of experimental results pertain to this mode. However, not only is this mode of fracture in itself of fundamental importance in the fracture of rocks in the earth, but in addition there is no obvious physico-chemical reason why the form of the law to describe processes such as stress corrosion, but not necessarily the parameters, should depend on mode (Das & Scholz 1981).

### MICROMECHANISMS OF FRACTURE

Following Ashby and others (Ashby *et al.* 1979, Gandhi & Ashby 1979) we can identify four main micromechanisms of tensile crack propagation for materials that cleave. I consider here only those mechanisms leading to

Presented to section 05 at the International Geological Congress, Paris, July 1980.

fracture after relatively modest plastic flow (less than 10%). Fractures forming after large strain (10–100%) without cleavage are not considered.

#### *Fracture controlled by pre-existing cracks*

A crack or a flaw in a brittle solid may propagate at stresses which are lower than that required for slip or twinning on any crystallographic system. No general plasticity is possible, but there may be local plasticity at the crack tip. Fracture occurs at a stress,  $\sigma_f$ , given by

$$\sigma_f \simeq \left( \frac{EG_c}{\pi c} \right)^{1/2} \quad (2)$$

where  $E$  is Young's modulus,  $2c$  is the pre-existing crack length and  $G_c$  is the critical strain energy release rate ( $G_c = K_I^2(1 - \nu^2)/E$  for plane strain, where  $\nu$  is Poisson's ratio). Gandhi & Ashby (1979) call this mechanism *cleavage 1*. Note that the fracture strength of a body is determined by the largest crack it contains.

#### *Fracture controlled by cracks generated through microplasticity*

If pre-existing cracks are very small or absent, then the stress can reach the level required to initiate slip or twinning. Provided that slip or twinning only occurs on a limited number of independent systems (less than 5) and the total bulk plastic strain is less than about 1% then internal stresses are generated which can nucleate cracks. This most commonly occurs when slip or twinning dislocations pile up at grain boundaries. Cracks that are nucleated in this way generally have a length which is proportional to the grain size,  $d$ , because this is the wavelength of the internal stresses. We can envisage that if the stress for twinning or slip on the softest system exceeds  $\sigma^*$  where

$$\sigma^* \simeq \left( \frac{EG_c}{\pi d} \right)^{1/2}, \quad (3)$$

then a crack will propagate as soon as it is formed and fracture will occur at the stress for the onset of microplasticity,  $\sigma_y$ . If, however,  $\sigma^*$  is greater than  $\sigma_y$ , then a crack nucleated by slip or twinning will not immediately propagate and the stress will have to be raised even further before macroscopic fracture occurs. Gandhi & Ashby (1979) call this mechanism *cleavage 2*.

#### *Fracture controlled by cracks generated through general plasticity/grain boundary sliding*

Substantial plastic strain (1–10%) precedes fracture by this mechanism which occurs on raising the temperature so that the flow stress falls to allow general plasticity or creep. Plasticity blunts small pre-existing cracks and effectively raises the resistance to fracture,  $G_c$ . Significant general plasticity or grain boundary sliding can then generate larger grain boundary cracks or cause a pre-existing crack to grow in a stable manner, until its

increased length, coupled with the higher stress caused by work-hardening force it to propagate unstably as a cleavage crack. Gandhi & Ashby (1979) term this mechanism *cleavage 3*.

Because of the delicate balance between the stress required to cause a mineral grain to cleave and the stress required to cause brittle grain boundary cracking it is not always an easy matter to predict which will predominate under any given set of conditions. This balance can be upset by small changes in temperature, impurity content, cement mineralogy and rock texture. The dominant fracture path is best determined by experiments. If brittle intergranular fracture occurs, then Gandhi & Ashby (1979) refer to it as *B.I.F.* 1, 2 or 3.

#### *Intergranular creep fracture*

Failure under high temperatures and low stresses is always by intergranular creep fracture (Gandhi & Ashby 1979). Voids or wedge cracks nucleate and grow (Söderberg 1972) on grain or phase boundaries. Nucleation is probably controlled by dislocation creep but when cracks are small growth is by local diffusion; the rate of diffusion being controlled by dislocation creep in the surrounding grains (Ashby *et al.* 1979). The linking of voids or cracks leads to a relatively low (less than 10%) ductility fracture after long periods of creep deformation.

#### *Fracture mechanism map*

Experimental results and theoretical descriptions of these fracture mechanisms can best be studied by constructing a fracture mechanism map as described by Ashby *et al.* (1979), Gandhi & Ashby (1979) and Dennis & Atkinson (1982). These maps are analogous to plastic flow deformation mechanism maps and indeed are partly based on them. They show the environmental conditions under which different mechanisms of fracture are dominant, i.e. produce failure in the shortest time.

Figure 1 is a typical fracture mechanism map for quartz. The method of constructing this figure and its key assumptions are given by Dennis & Atkinson (1982). Note, however, that the top of Fig. 1 is truncated by the stress required to overcome the interatomic forces in a perfect crystal. This is given by

$$\sigma_{\text{ideal}} = E/10. \quad (4)$$

At the highest stresses lies the field of dynamic fracture which is the region where even the initial loading must be described in terms of the propagation of an elastic wave through the material.

Contours of time-to-failure or crack velocity could have been superimposed on the map but the paucity of data precludes such a refinement at this stage.

One may infer from the fracture mechanism map that for the upper 20 km, or so, of the earth's crust, cleavage (*B.I.F.*) 1 will be the most important fracture mechanism. For this reason I will concentrate on this mechanism in the ensuing discussion.

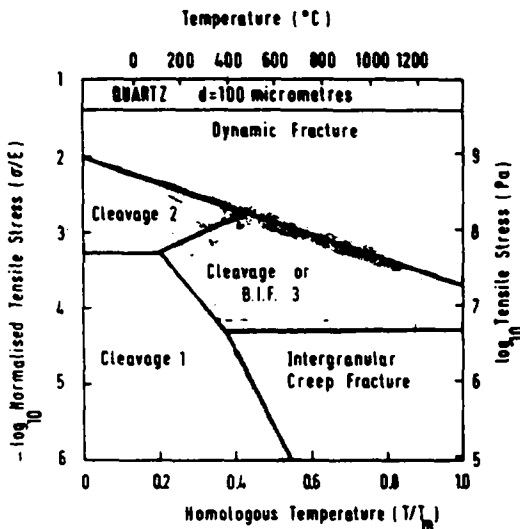
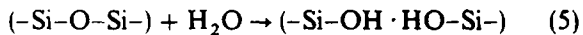


Fig. 1. Fracture mechanism map for quartz. Normalized tensile stress is plotted against homologous temperature. Grain size is 100 micrometres.

#### Influence of chemical effects on fracture

There are a number of different ways in which the action of the environment or the chemistry of the phases involved can help lower the barriers to crack propagation. Consider the influence of these variables on cleavage/B.I.F. 1 in quartz.

(a) The presence of liquid water, water vapour or some other reactive species in the crack tip environment can facilitate crack propagation by promoting weakening reactions. For the quartz/water system reactions of the form



may occur. The strong silicon-oxygen bonds are replaced with much weaker hydrogen bonds (Scholz 1972, Martin 1972, Swain *et al.* 1973, Atkinson 1979, Atkinson & Meredith 1981). This phenomenon is known as stress corrosion.

(b) Some solids contain dissolved chemical impurities, such as structurally bound water in quartz, which can have a degrading effect on strength if present in sufficient quantities. During crack propagation stress directed diffusion of these chemical impurities to crack tips may occur, where they can take part in weakening reactions, thus facilitating crack extension (Schwartz & Mukherjee 1974). In addition, the difference in chemical potential between the highly stressed atoms of the crack tip and those in the bulk of the solid can lead to a concentration gradient of vacancies at the crack tip. The diffusion of vacancies to the crack tip will then control the crack propagation rate as described by Stevens & Dutton (1971). These diffusion-based mechanisms are only likely to be important, however, at relatively high homologous temperatures.

(c) If the chemical environment contains species which can undergo ion exchange with species in the solid phase, and if there is a gross mis-match in the size of these different species then lattice strains can result from ion

exchange which can facilitate crack extension, e.g. exchange of  $\text{H}^+$  for  $\text{Na}^+$  in silicate glasses (Wiederhorn 1978).

Atkinson (1979) has suggested that for quartz at least the most important of these effects is stress corrosion at low homologous temperatures. The overwhelming proportion of data on subcritical crack propagation in rocks relates to this phenomenon. I shall concentrate on this aspect of subcritical crack propagation in the rest of this paper.

### THEORETICAL BACKGROUND TO STRESS CORROSION

Observations on stress corrosion in a wide range of glasses, oxides and silicates are broadly consistent with a schematic stress intensity factor ( $K_I$ )/crack velocity ( $v$ ) diagram shown in Fig. 2 for mode I crack propagation.

In this diagram  $K_{Ic}$  is the critical stress intensity factor and  $K_0$  is a threshold stress intensity factor below which no appreciable crack growth occurs.  $K_0$  is not commonly observed even at very low velocities, but consideration of the properties of materials suggests it must exist. In region 1,  $v$  is apparently controlled by stress corrosion reactions. At higher  $K_I$  values in region 2 the transport of reactive species to the crack tip is believed to be rate controlling. At yet higher  $K_I$  values  $v$  is controlled by some poorly understood, thermally activated process that is comparatively (but not totally) insensitive to the chemical character of the environment.

The influence of increasing the partial pressure or concentration of water in the environment is shown in Fig. 2. Increasing temperature also tends to shift the  $K_I$ - $v$  curves towards the top left hand of the diagram. The influence of hydrostatic pressure is not known. It might be expected that increasing the pressure on a water-bearing

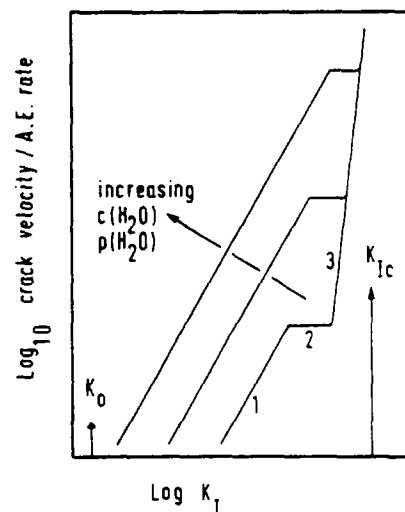


Fig. 2. Schematic stress intensity factor ( $K_I$ )-crack velocity ( $v$ ) curves. The threshold stress intensity factor ( $K_{I0}$ ) and the critical stress intensity factor ( $K_{Ic}$ ) are shown. For an explanation of the significance of regions 1, 2 and 3 see text.

environment would enhance the rate of stress corrosion because the water molecules become more concentrated and chemical corrosion reactions are enhanced. The limited evidence available from work on metals (Dehart & Liebowitz 1968), however, suggests that in some materials, at least, stress corrosion is suppressed by pressure. In some cases  $K_0$  may be increased by application of pressure (Gerberich 1974). Furthermore, Kranz's (1980) study of the influence of pressure on static fatigue of granite can be interpreted to show that increasing pressure decreases the rate of stress corrosion primarily by increasing the activation enthalpy required for the stress corrosion process. Secondary effects might include a retardation of the rate at which corrosive species can reach crack tips by decreasing crack-wall spacing under pressure.

It is worth noting that even for silicate glasses the stress corrosion explanation for the schematic  $K_1-v$  curves of Fig. 2 is not universally accepted. Marsh (1964), Wiedmann & Holloway (1974) and Williams & Marshall (1975) have suggested that plastic flow may be an alternative explanation, even at ambient temperatures. The latter two authors have attempted to put their ideas into quantitative form. However, it has yet to be shown that the theories of Wiedmann & Holloway (1974) and Williams & Marshall (1975) are consistent with the huge volume of data on the environmental dependence of crack velocity even in silicate glasses. Until then these ideas should be viewed with caution, especially in the light of the marked success of chemical theories of fracture (see later) in accounting for experimental observations of environmentally dependent subcritical cracking (Wiederhorn 1974, 1978). Moreover, even allowing that plastic flow may be of minor significance in low-temperature subcritical cracking of some minerals, such as calcite or galena, all the available evidence (Martin & Durham 1975, Dunning *et al.* 1980) suggests that low-temperature subcritical crack propagation in quartz is not accompanied by significant plastic flow.

There have been numerous attempts to develop theoretical descriptions of  $K_1-v$  curves in terms of chemically assisted stress corrosion processes. The early theories have been reviewed by Anderson & Grew (1977) and will not be repeated here (see also Atkinson 1979). I will concentrate on the most widely used expressions and those that have been most recently published.

The two most commonly used equations to describe stress corrosion data are Charles' (1958) power law

$$v = v_0 \exp(-\Delta H/RT) K_1^n \quad (6)$$

and the Wiederhorn & Bolz (1970) equation

$$v = v'_0 \exp[(-\Delta H + 2V^*K_1)/(\pi\rho)^{1/2}]/RT \quad (7)$$

where  $v$  is the crack velocity,  $v_0$  and  $v'_0$  are pre-exponential factors,  $\Delta H$  is an activation enthalpy,  $V^*$  is an 'activation volume',  $\rho$  is the radius of curvature of the crack tip,  $R$  is the gas constant,  $n$  is a material constant known as the stress corrosion index, and  $T$  is the absolute temperature. Equation (7) is based on the Charles & Hillig (1962)

formulation for stress corrosion which, in turn, is based upon reaction rate theory and continuum mechanics. Empirical data on stress corrosion are often fitted to the equation

$$v = v'_0 \exp(-\Delta H + \beta K_1)/RT \quad (8)$$

where  $\beta$  is an experimentally determined constant and equation (8) is identical with equation (7) when  $V^* = (\beta/2)(\pi\rho)^{1/2}$ .

Although (6), (7) and (8) have been widely used in studies of glasses and ceramics, the Charles equation (6) has been used most often in studies of rocks and minerals. In part this is because the Wiederhorn & Bolz equation can only be used to describe region 1 of the schematic  $K_1-v$  curve. Charles' equation on the other hand can be used with appropriate changes in  $v_0$ ,  $\Delta H$  and  $n$ , to describe all three regions of the schematic  $K_1-v$  curve. Furthermore, these two theories of stress corrosion are still largely empirical and because  $n$  in (6) is often large (usually  $> 10$ ) then it is virtually impossible in practice to distinguish between (6) and (8).

In an attempt to model chemically-enhanced subcritical cracking at the atomic level Lawn (1975) and Lawn & Wilshaw (1975) developed a two-stage description of crack propagation in which reactive species must first be transported to the crack tip before reactions can occur there to facilitate crack extension. The slowest of these two steps, reaction and transport, will control the rate of the overall process. The central idea in crack advance is of an ideally brittle fracture crack in which sequential bond rupture occurs via the lateral motion of atomic kinks along the crack front. For the case when solid/vapour reactions limit the crack velocity ( $v_r$ ) Lawn found that

$$v_r = V(T) \left[ \frac{p_a^0}{p_a^s} \right]^{\eta/2} \exp(-U_0^*/kT) \exp(G/2N_s kT) \quad (9)$$

where  $G$  is the strain energy release rate,  $V(T)$  is a slowly varying temperature-dependent term,  $p_a^0$  is the vapour pressure at the crack mouth,  $p_a^s$  is the vapour pressure in some reference state,  $\eta$  is the number of molecules of environmental species reacting with one bond in the solid to produce a weakened state,  $U_0^*$  is a collection of various uncertainty energy constants,  $k$  is Boltzmann's constant, and  $N_s$  is the surface density of crack plane bonds. For transport-limited crack velocity ( $v_t$ ) Lawn (1975) obtains

$$v_t = \kappa a_0 p_a^0 / \eta N_s (2\pi m k T)^{1/2} \quad (10)$$

where  $\kappa$  is an attenuation factor associated with the increasing incidence of retarding, diffuse molecule wall collisions as the gas approaches the crack tip,  $a_0$  is the lattice spacing, representing the reaction cross-section per unit width of crack front presented to the impinging gas molecules by the crack tip bonds and  $m$  is the molecular mass of the gaseous species.

Equations (9) and (10) can account quite well for stress corrosion crack growth in the sapphire/water vapour system (Lawn 1975). As it stands, however, Lawn's atomistic theory would not be able to account for more complex behaviour, such as shown by polycrystalline,

polyphase ceramics and rocks, or more complex chemical effects. In principle, however, Lawn's approach can be extended to include these more complex phenomena. It becomes necessary to rewrite the total energy function of the system to suit the appropriate new system variables and to identify the various mechanisms which contribute to the overall crack growth process, and then to determine the conditions under which each mechanism might assume a rate-controlling role.

Brown (1979) has recently taken the analysis of subcritical crack growth an important stage further. He noted that no existing theory can account in a unified manner for all three stages of the schematic  $K_I-v$  curve. Approaching the problem of slow crack growth in terms of steady state multibarrier kinetics (network theory) he derived a general equation that does account for all three regions of a  $K_I-v$  curve and from which specialized expressions can be developed for the crack velocity in specific cases.

From the hypotheses that (a) subcritical crack growth consists of  $l$  competitive rate processes, each of which is composed of  $n_j$  sequential steps ( $j = 1, 2, 3, \dots, l$ ) and (b) the crack advances by the generation and movement of double kinks along the crack front, which itself is more like a band, a number of kink steps wide, than a line, Brown (1979) obtains

$$v = \# \lambda_k^2 (kT/h) \sum_{j=1}^l \left\{ \frac{1 - \exp(\Delta G_j/RT)}{(c_{1,j}k/h) + \sum_{g=2}^{m_j} [\theta_{g,j} a_{g,j} \exp(\Delta G_{g,j}^*/RT)]} \right\} \quad (11)$$

where  $\#$  is the steady state number of active double kinks per unit length of crack band,  $\lambda_k$  is the average step size of a double kink, and  $h$  is Planck's constant. The set of  $n_j$  sequential steps is perceived as a collection of  $m_j$  sequential subsets each of which corresponds uniquely to a different rate process in the series.  $\theta_{g,j}$  = the number of sequential steps corresponding to the  $g$ th subset both in the  $j$ th set.  $a_{g,j}$ 's are dimensionless parameters which lump appropriate geometric factors, reactant concentrations raised to the powers of their respective orders of reaction, stoichiometric constants and conversion factors corresponding to the  $g$ th subset of the  $j$ th sequence.  $\Delta G_{g,j}^*$  are the Gibbs free energies of activation for forward steps in the  $g$ th subset.  $(-\Delta G_j)$  is the free energy driving force for the entire  $j$ th sequence.  $c_{1,j}$  is a parameter that relates to gaseous diffusion processes (transport of reactive species to crack tip through an interadjacent, stagnant gas film) where one  $m_j$  is arbitrarily designated the subset for which  $g = 1$ . It depends on thickness of the stagnant gas film, the order of the stress-sensitive bond-rupturing reactions, the collision cross section and molecular weight of both reactant species and inert gas species, Avogadro's number, the mole fraction of reactant species and the average step size of a double kink.

Equation (11) is very general and was specialized for selected cases in order to obtain  $v = v(K)$  relations. To do this, odd  $j$  suffixes were arbitrarily assigned to those

sequences which include mass transport of a key reactant or product species between the environment and crack tip. Even  $j$  suffixes correspond to those processes that occur wholly within the solid, at and/or near the crack tip, that are comparatively unaffected by the environment,  $l$  is set  $< 4$ . Subcritical crack growth was classified according to five general environments: (1) inert gas or liquid, or vacuum, (2) dilute reactive gas, (3) dilute reactive liquid, (4) concentrated reactive gas and (5) concentrated reactive liquid. The number of  $v = v(K)$  relations that can be obtained from equation (11), even with  $l \leq 4$  is enormous, but study of a wide range of empirical data suggests that certain simplifications are possible. A specific expression for  $v = v(K)$  that fits a wide variety of mechanisms and types of environment was found by Brown (1979) to be

$$v = \Omega_0 \exp(\Omega_1 K_I) + \frac{\Omega_2 \exp(\Omega_3 K_I) \{1 - \exp[-L(K_I - K_I^*)]\}}{1 + \Omega_4 \exp(\Omega_3 K_I)} \quad (12)$$

where  $K_I$  is the mode I stress intensity factor,  $K_I^*$  is a threshold stress intensity factor,  $L$  is a constant and the  $\Omega$ 's are lumped constants that have theoretic definitions that correspond to specific cases and conditions. For more details see Brown (1979). One advantage of this approach is that many different transport mechanisms to the crack tip can be included in  $\Omega_4$ , for example, stress independent, bulk, solid state diffusion or surface diffusion.

For many materials where values can be assigned to the constants  $\Omega$ , such as porcelain in water, soda-lime-silicate glass in octanol, there is excellent agreement between the theory and experimental results for all three regions of the  $K_I-v$  curve. However, to assign values to the constants  $\Omega$  can be a formidable task and at least at present is not really feasible for studies of rocks. Although Brown's (1979) theory clearly has substantial scope for future application in geophysics there is at present too much guesswork involved in assigning values to the constants in (12) for rocks.

Thomson has recently developed Lawn & Wilshaw's (1975) ideas a stage further (Thomson 1980, Fuller & Thomson 1980) and attempted to provide a more satisfactory theoretical framework. He addresses the problem of fracture at an atomically sharp crack assisted by the adsorption of a gaseous chemical species which lowers the energy of bond breaking. He obtained a general statistical mechanical description of brittle crack growth in terms of chemical absolute reaction rate theory that leads to certain general conclusions. The most important one is that chemically assisted fracture should be a widespread phenomena, associated with the lowering of the surface energy of the material by the external environment. However, steric or size effects can restrict the external molecules from entering the cohesive region where chemical reactions occur and a variety of complex chemical effects can occur at a crack tip to strengthen the crack or to slow down its growth. Thus the details of environmentally-assisted fracture will vary widely from one system to another. Despite the enormous literature on fracture there

is little in the way of an appropriate data base with which to check the specific quantitative predictions of Thomson and to throw light on the specific chemical processes involved.

Krausz (1978) has developed a theory of stress corrosion cracking based on deformation kinetics theory that amplifies some aspects of Lawn & Wilshaw's (1975) work and anticipates some of Brown's (1979) conclusions. This chemical kinetic approach shows that regions 1 and 2 of the schematic  $K_I$ - $v$  curve are associated with two consecutive energy barriers in parallel with a single energy barrier associated with region 3 behaviour. He obtained the following expression for the crack velocity

$$v = n_c a \frac{1 - \frac{kT}{h} ({}_1k_1)^{-1}}{\{k(1)\}^{-1} + \{k(2)\}^{-1}} + n_p a_0 k(3) \quad (13)$$

where  $k(1)$ ,  $k(2)$  and  $k(3)$  are the single rate constants that describe the behaviour in regions 1, 2 and 3. These must be determined by theoretical analysis in conjunction with appropriate experiments to clarify which of the rate constants associated with the forward or backward consecutive barriers in regions 1 and 2 actually dominate  $k(1)$  and  $k(2)$  for specific combinations of material and environment. At each bond-breaking event the crack will propagate by a multiple integer ( $n_c$ ) of the atomic distance ( $a_0$ ).  $m_p$  is the number of bonds broken in unit crack advance during the region 3 mechanism and this may be different to that during crossing of the consecutive energy barrier,  $n_c \cdot {}_1k_1$  is an elemental rate constant associated with the threshold region barrier.

One interesting conclusion of Krausz's work is that as long as the mechanism of the consecutive processes in regions 1 and 2 does not change, then the threshold stress intensity is independent of temperature.

I have already alluded to the suggestion of Stevens & Dutton (1971) that at relatively high homologous temperatures slow crack growth in some materials may be facilitated by mass transport processes such as volume or surface diffusion or vapour phase transport. For example, Stevens & Dutton (1971) show that surface diffusion and vapour phase transport may control the high-temperature static fatigue of alumina in a dry environment, even though at low temperatures in water vapour crack propagation may well be controlled by stress corrosion. Unfortunately, there are too few experimental data points to constrain the theoretical predictions for ceramics. There is no pertinent data for rocks. However, the general implication of Stevens & Dutton's work, that mechanisms of fracture are dominant over different ranges of environmental conditions, is entirely consistent with the view of fracture that I have sought to present in this article.

Unfortunately, the more recent of theories described in this section are only easily applicable to certain simple, model systems such as soda-lime silicate glass/water or alumina/water. The complexities of subcritical cracking in polyphase, polycrystalline rocks which have complicated microstructures, cements, fabrics and chemistry at present cannot easily be analysed in these terms. A full description

of subcritical cracking of rocks in terms of fundamental processes is certain to be highly complex. Evans & Graham (1975) have used acoustic emission amplitude studies to construct a model of macro crack propagation in single phase polycrystalline ceramics that takes into account some of the complexities of microstructure, but this sort of work is still in its infancy.

Under these circumstances, and considering the relatively limited data available on subcritical cracking of rocks compared to that of model materials, such as silicate glasses, the continued use is justified of the relatively simple and semi-empirical Charles power law (6) to describe stress corrosion results for geological materials. Not only has this equation certain advantages (described above) but it is also the equation that is most often favoured by experimentalists who have studied stress corrosion in rocks.

## EXPERIMENTAL STUDIES OF STRESS CORROSION IN GEOLOGICAL MATERIALS

### Quartz

Static fatigue of quartz in wet environments was studied by Scholz (1972), Martin (1972) and Martin & Durham (1975), but their results were not reported in terms of fracture mechanics parameters. Swain *et al.* (1973) explored the influence of water on the strength of quartz in Hertzian indentation experiments.

Atkinson (1979) was the first to report stress corrosion data on quartz (Table 1) in terms of  $K_I$ - $v$  diagrams, obtained using the double torsion testing method. Crack growth rates as slow as  $10^{-9} \text{ m s}^{-1}$  were studied without any firm evidence of a stress corrosion limit. All of Atkinson's data pertain to region 1 of the schematic  $K_I$ - $v$  curve (Fig. 2). Using the theory of Lawn (1975) a plateau (region 2) in the  $K_I$ - $v$  curve for quartz was calculated to lie at  $4 \times 10^{-4} \text{ m s}^{-1}$ , in good agreement with experimental observations (Fig. 3). Bruner (1980a) obtained additional  $K_I$ - $v$  data on quartz, but by using double cantilever beam specimens. As is shown in Fig. 3 crystallographic orientation can clearly exert a pronounced influence on crack propagation rates in this material, especially at slow crack velocities. This point was also inferred by Scholz (1972) from his static fatigue experiments.

Atkinson & Meredith (1981) have shown that at room temperature the pH of the aqueous environment can strongly influence the rate of crack propagation at low values of  $K_I$  but this influence diminishes as  $K_I$  is raised (Fig. 4). At very high values of  $K_I$  close to  $K_{Ic}$  no significant influence of pH on crack propagation rates is observed. This is interpreted in terms of a two stage model as follows. At low crack velocities the crack tip environment is open to modification by the external environment through the diffusion of chemical species along the crack between the bulk fluid and the crack tip. Chemical differences between the crack tip and the bulk fluid are not long sustained and the crack tip environment is controlled

Table 1. Compilation of stress corrosion parameters ( $n$ -stress corrosion index, and activation enthalpy for crack propagation) in geological materials

Material	Conditions	Activation enthalpy (kJ mole <sup>-1</sup> )	Stress corrosion index ( $n$ )	Reference
quartz				
$a$ plane $\perp r$	air, 30% r.h., 20°C		19.9	Atkinson (1979)
$a$ plane $\perp z$	water, 20–80°C	52.5	12.0	Atkinson (1979)
	2N NaOH, 20°C		9.5	Atkinson/Meredith (1981)
	2N HCl, 20°C		19.3	Atkinson/Meredith (1981)
5° to {0110}	water vapour, 90–240°C	108		Martin (1972)
	water vapour, 20–250°C	63		Martin/Durham (1975)
$\langle c \rangle$	water vapour, 20–50°C	46–100		Scholz (1972)
Arkansas novaculite	water, 20–80°C	69.5	25.1	Atkinson (1980)
Falerans micrite	air, 20°C		~130	Henry/Paquet (1976)
	water + CaCO <sub>3</sub> , 20°C		26	Henry/Paquet (1976)
	water + CaCO <sub>3</sub> , 20–85°C	63–147		Henry (1978)
St. Pons. marble	water + CaCO <sub>3</sub> , 20°C		26–29	Henry/Paquet (1976)
Black gabbro	air, 30% r.h., 20°C		32.1	Atkinson/Rawlings 1979, 1981
	water, 20°C		36.1 (region 3) 28.6 (region 1)	op cit. op cit.
Murata basalt	air, 20°C		22	Sano/Ogino (1980)
Ralston intrusive	air, 28% r.h., 20°C		44.4	Atkinson <i>et al.</i> (1980)
	water, 20°C		23.5	Atkinson <i>et al.</i> (1980)
Kinosaki basalt	air, 30°C		~34	Waza <i>et al.</i> (1980)
	water, 25°C		~33	Waza <i>et al.</i> (1980)
Whin Sill dolerite	air, 30% r.h., 20°C		31.2	Meredith/Atkinson (1981)
	water, 20–80°C		29	Meredith/Atkinson (1981)
Westerley granite	air, 30% r.h., 20°C		39.1	Atkinson/Rawlings (1981)
	water, 20°C		34.8	Atkinson/Rawlings (1981)
	air, 30% r.h., 20°C		35.9	Atkinson <i>et al.</i> (1980)
	water, 20°C		33.7	Atkinson <i>et al.</i> (1980)
	toluene, 11.3% r.h.		51	Swanson (1980)
	water, 20°C		53	Swanson (1980)
Oshima granite	air, 20°C		30	Sano/Ogino (1980)
Yugara andesite	air, 25°C		~31	Waza <i>et al.</i> (1980)
	water, 25°C		~26	Waza <i>et al.</i> (1980)
Lac du Bonnet granite	air, 20°C		58.5	Wilkins (1980)
	air, 20°C		55.9	Wilkins (1980)

by the chemical composition of the bulk fluid. At high crack velocities ( $c. 10^{-2} \text{ m s}^{-1}$ ) transport of chemical species from the bulk fluid to the crack tip environment cannot keep pace with the creation of new sources of reactive ions in fresh crack surfaces. In this case the composition of the crack tip solution is controlled primarily by the chemical composition of the fresh crack surfaces. The greater the availability of OH<sup>-</sup> ions, the faster is the rate of crack propagation, for a given value of  $K_I$ .

As mentioned earlier, electron microscope studies (Martin & Durham 1975, Dunning *et al.* 1980) have shown that chemically enhanced crack growth is not accompanied by any significant plastic deformation, at

least at temperatures up to 250°C. In Martin & Durham's (1975) study, however, Dauphiné twins were observed in experiments at 125°C and above. It is possible that Dauphiné twins are produced in advance of crack propagation in contact-loaded quartz (see Hartley & Wilshaw 1973) but the very small atomic motions that this involves serve merely to efficiently accommodate the local elastic strain that accumulates in elastically anisotropic quartz.

Hartley & Wilshaw (1973) have interpreted their Hertzian indentation studies to show that intrinsic water in the quartz structure may promote strength reduction at temperatures above 520°C by stress-assisted diffusion of lattice water to crack tips. The role of OH<sup>-</sup> ions in the

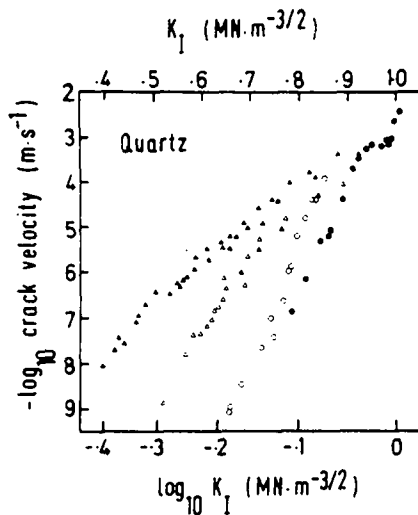


Fig. 3. Synoptic diagram showing the influence of crystallographic orientation on stress corrosion in quartz. Stress intensity factor is plotted against  $\log_{10}$  of crack velocity. After Bruner (1980a). Solid and open circles are for crack growth on  $r$  in the direction  $\{10\bar{1}2\}$  for 2 specimens of natural quartz at 62.5% r.h. (Bruner 1980a). Solid triangles are for crack growth perpendicular to  $z$  on  $a$  in synthetic quartz in liquid water (Atkinson 1979). Open triangles are for crack growth perpendicular to  $r$  on  $a$  in synthetic quartz at 68% r.h. (Atkinson 1979).

silica lattice, however, is markedly affected by annealing.

No systematic attempt has been made here to identify data pertaining to synthetic or natural quartz. There is some suggestion, however, that some types of natural Brazilian quartz may have markedly different fracture properties to synthetic quartz (Norton & Atkinson 1981).

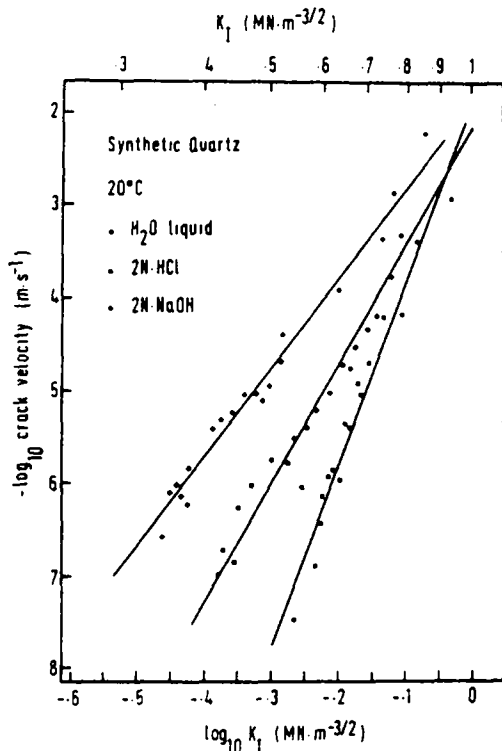


Fig. 4. Influence of environment chemistry (pH) on crack propagation in synthetic quartz. Crack growth occurs on the  $a$  plane in a direction normal to  $z$ .  $\log_{10}$  of stress intensity factor is plotted against  $\log_{10}$  of crack velocity. After Atkinson & Meredith (1981).

### Quartz rocks

$K_I$ - $v$  data for double torsion specimens of Arkansas novaculite (Table 1) in liquid water at 20–80°C have been published by Atkinson (1980). Crack velocity data were obtained in the range from  $10^{-4}$  to  $10^{-10}$   $\text{m s}^{-1}$ . All data pertain to region 1 of the schematic  $K_I$ - $v$  curve and no stress corrosion limit was observed.

Stress corrosion effects have been invoked by Peck (1980) to explain a 15–20% reduction in fracture energy when double cantilever beam specimens of Sioux quartzite were tested in tap water rather than in air.

### Calcite rocks

Henry (1978) and Henry & Paquet (1976) have reported stress corrosion data for double torsion specimens of marble and a micrite in liquid water containing dissolved  $\text{CaCO}_3$ , and in moist air (Table 1). The slopes of  $K_I$ - $v$  diagrams for marble were not much influenced by orientations, although the values of  $K_I$  were. These data for calcite rocks do not show the simple trimodal pattern familiar from work on silicate glasses. As  $K_I$  was lowered at the slow-velocity-end of region 1 behaviour there appeared a second, constant crack velocity, plateau region followed at still lower  $K_I$  values by another region where crack velocity decays with  $K_I$  at much the same rate as for region 1 behaviour. This apparently anomalous region may be ascribed to relatively poor data obscuring a threshold stress intensity. Alternatively, if the effect is real then it may result from complex chemical reactions between solid and solution or to the onset of plastic deformation as a contributor to crack growth processes.

For a given stress intensity factor the rate of crack propagation in micrite is generally increased on raising the pH of the corrosive medium above 7 (Henry 1978).

### Basaltic rocks

To date, all experiments run on basaltic rocks have used the double torsion testing method (Fig. 5, Table 1).

Crack growth in Black gabbro was followed by Atkinson & Rawlings (1979, 1981) down to velocities of  $c. 10^{-9}$   $\text{m s}^{-1}$  ( $0.54 K_{Ic}$ ) without encountering a stress corrosion limit. Waza *et al.* (1980) studied subcritical crack propagation in relatively porous (6%) Kinosaki basalt. The porous nature of the basalt may explain why it was apparently much weaker ( $K_{Ic} = 1.1 \text{ MN m}^{-3/2}$ ) than the coarser grained Black gabbro ( $K_{Ic} = 2.9 \text{ MN m}^{-3/2}$ ).  $K_{Ic}$  for Murata basalt is in excess of  $2 \text{ MN m}^{-3/2}$  (Sano & Ogino 1980). Stress corrosion data for Whin Sill dolerite have been determined by Meredith & Atkinson (1981).

Crack velocity- $K_I$  curves for a lunar analogue basaltic glass at water vapour pressures of 1.33 kPa and 0.13 Pa show that increasing water pressure at constant  $K_I$  dramatically enhances the crack velocity (Soga *et al.* in press). The basaltic glass was made from Ralston intrusive. Stress corrosion data for the crystalline form of this rock are given by Atkinson *et al.* (1980).



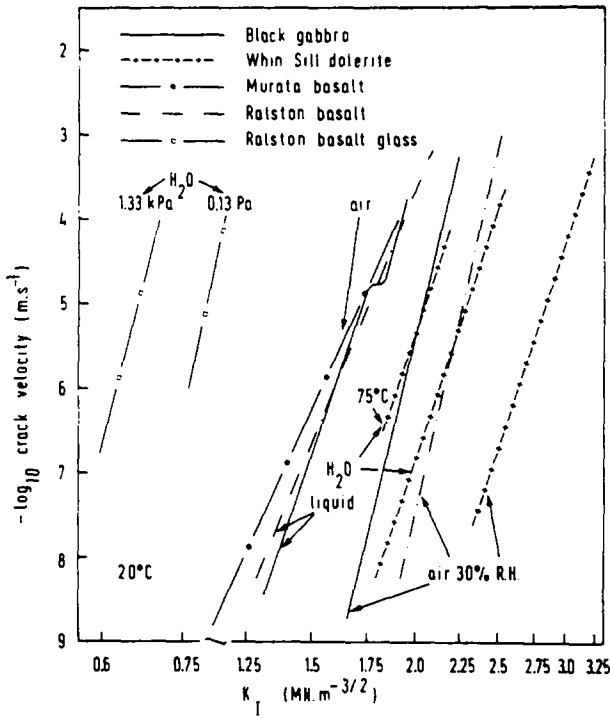


Fig. 5. Synoptic  $K_1-v$  diagram for rocks of basaltic composition. Note discontinuous stress intensity factor scale. All tests at 20°C unless otherwise indicated.

Granitic rocks

Figure 6 shows a synoptic diagram of most of the available stress corrosion data for granitic rocks. Values of the stress corrosion index and testing conditions can be found in Table 1. With the exception of Wilkins' (1980) fracture statistics approach, all other workers on granitic

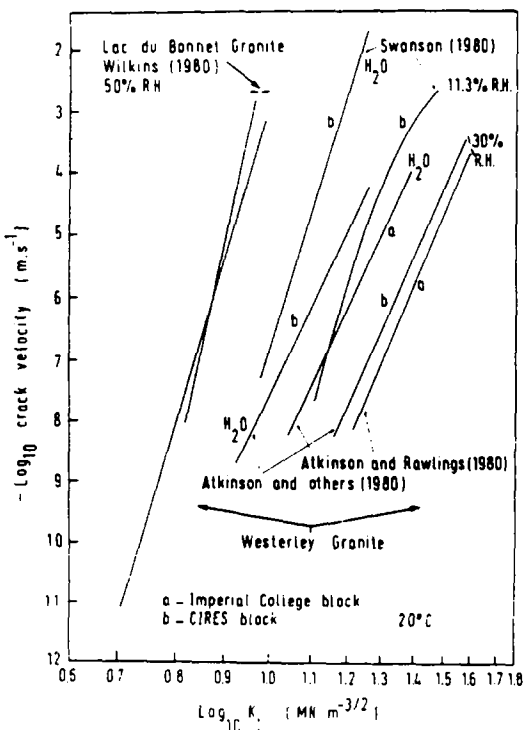


Fig. 6. Synoptic  $K_1-v$  diagram for rocks of granitic composition. All tests at 20°C.

rocks have used the double torsion method. One especially interesting feature of Fig. 6 is the absence of a stress corrosion limit in Lac du Bonnet granite even at crack velocities as slow as  $10^{-11} \text{ m s}^{-1}$ .

It can be inferred from Swanson's (1980) data for Westerley granite in toluene that as crack velocity is raised above approximately  $10^{-3} \text{ m s}^{-1}$  there is a gentle reduction in the slope of the  $K_1-v$  curve. This could mean that region 2 behaviour (see schematic  $K_1-v$  curve, Fig. 2) is being approached. The gentle slope change observed for granite contrasts with the rather abrupt change noted for silicate glasses and some ceramics. Because the crack 'tip' in granite consists of many secondary cracks at these velocities (Swanson 1980) the gradual change in slope may be explained as a result of the differential onset of region 2 behaviour for different secondary cracks. The conditions for the onset of this behaviour will depend on crystallographic orientation, on the nature of the host mineral, and on the degree of intra- and inter-granular character to the crack path.

There is some spread in the range of results for Westerley granite. This is probably due to differences in testing techniques because when different blocks of Westerley granite are tested in the same laboratory using identical testing techniques then relatively similar results are obtained. For example, compare curves labelled a and b in Fig. 6 for air of 30% r.h. (Atkinson & Rawlings 1981; Atkinson *et al.* 1980). The uncertainty in measuring  $K_1$  and  $v$  is approximately 2.5 and 15%, respectively.

Microscopic studies of the crack path during stress corrosion in Westerley granite have shown that there is a decrease in the ratio of transgranular to intergranular fracturing as crack propagation rates are reduced (Swanson 1980, Atkinson & Rawlings 1981).

Other geological materials

Time-to-failure tests have been conducted by Schmidt (1976) on oil shale from Anvil Points Colorado in distilled water, air of 7% r.h. and in dry argon. Schmidt concluded that stress corrosion can reduce the time-to-failure in this material provided that  $K_1$  is greater than  $0.8 K_{Ic}$ . Because these tests never lasted for longer than 123 h it is of course possible that stress corrosion can occur at yet lower levels of  $K_{Ic}$ , but at rates which are so slow that failure will result after weeks, months or years rather than a few hours.

Wiederhorn (1968) has obtained  $K_1-v$  curves for stress corrosion of  $\{10\bar{1}2\}$  fractures in sapphire in the presence of water vapour. These data spanned a range of velocities from  $10^{-8}$  to  $10^{-4} \text{ m s}^{-1}$  and showed all the features of the schematic  $K_1-v$  curve (Fig. 2). The most striking aspect of the data is that the plateau, or transport-controlled region (region 2) is shifted dramatically to higher crack velocities on raising the pressure of water vapour. For example, region 2 behaviour occurs at  $c. 7 \times 10^{-7} \text{ m s}^{-1}$  under water vapour pressures of  $2.4 \text{ N m}^{-2}$ , but on raising the pressure to  $300 \text{ N m}^{-2}$  region 2 is shifted to  $c. 7 \times 10^{-5} \text{ m s}^{-1}$ . Lawn's (1975) atomistic theory can account for the qualitative features of these results on sapphire.

### Acoustic emission and stress corrosion

A substantial body of literature exists on acoustic emissions during subcritical crack growth in ceramics (e.g. Evans & Linzer 1973). These transient elastic waves often have frequencies between 100 kHz and 1 MHz. A few years ago Anderson & Grew (1977) surveyed the available literature and arrived at the conclusion that experiments had not yet satisfactorily answered the question of whether rocks undergo slow crack growth without acoustic emission. Since that time there have been a number of reports that have shown clearly that not only do rocks show acoustic emission during stress corrosion, but that the characteristics of these emissions can be related to the mechanisms of crack growth and hence to parameters such as stress intensity factor, crack velocity and the 'humidity' at the crack tip. Acoustic emission, therefore, is an excellent means of remotely monitoring the characteristics of stress corrosion crack growth in rocks.

In an early study, Scholz (1972) showed that the rate of microfracturing, estimated from the rate of acoustic emission, of single crystals of quartz is proportional to crack velocity. Byerlee & Peselnick (1970), however, were unable to detect with their instruments acoustic emission from slow crack growth in glass.

Atkinson & Rawlings (1979, 1981) have made an extensive study of acoustic emission during stress corrosion in double torsion plates of Westerley granite and Black gabbro. Acoustic emissions were observed in the range of frequencies from 100 kHz to greater than 1 MHz. A spectral peak occurred in the region of 200 kHz and so further monitoring of emissions was restricted to the bandwidth 100–350 kHz. In both granite and gabbro significant acoustic emission accompanies crack propagation at even the slowest crack velocities observed ( $10^{-9} \text{ m s}^{-1}$ ). The acoustic emission rate was directly proportional to the crack velocity and could be used as an indirect measure of this parameter. For example, see Fig. 7. In addition, amplitude distributions, measured by the parameter  $b$ , show distinctive shifts with increase in stress (see Fig. 8). The amplitude distribution parameter,  $b$ , is given by

$$n(V) = (V/V_0)^{-b} \quad (14)$$

where  $n(V)$  is the fraction of the emission population whose peak amplitude exceeds amplitude  $V$ , and  $V_0$  is the lowest detectable amplitude. Furthermore, both the acoustic emission rate and the amplitude distribution are sensitive to the details of the mechanism of crack propagation which is controlled by stress intensity factor and crack tip 'humidity.'

An especially interesting feature of Fig. 8 is that the trends in the amplitude distributions do not seem sensitive to rock type.

Swanson (1980) has used acoustic emission location techniques to pin-point the source of emissions in double torsion tests on Westerley granite. He found that subsidiary microcracking ahead of the main fracture occurred at crack velocities greater than  $10^{-5} \text{ m s}^{-1}$ , but not at

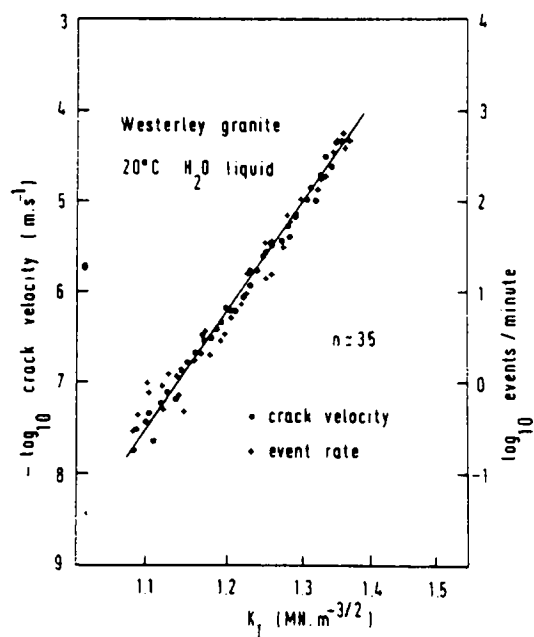


Fig. 7. Plot of crack velocity ( $v$ ) and acoustic emission event rate ( $dN_E/dt$ ) against mode I stress intensity factor ( $K_I$ ) for Westerley granite in liquid water at 20°C.

lower velocities. Both macrocrack and microcrack extension was probably controlled by stress corrosion. The results of Atkinson & Rawlings (1981) can be interpreted to show that the majority of acoustic emission from crack growth in double torsion plates of Westerley granite and Black gabbro over the range of velocities  $10^{-4}$  to  $10^{-9} \text{ m s}^{-1}$  occurs by extension of the macrocrack.

Sano & Ogino (1980) have also noted that acoustic emission rate in rock shows a close relation with the growth rate of cracks in double torsion plates. They studied the behaviour of Murata basalt and Oshima granite. In these studies a tendency was observed for the dominant frequency (in the range 100 kHz to 1 MHz) to decrease with increase in crack velocity. In contrast to this, acoustic emission studies during uniaxial compressive experiments on Ralston intrusive (basalt), Westerley granite and pyrophyllite showed an enhancement of high frequency spectral components in events prior to failure, i.e. as stress or crack velocity increases (Granryd *et al.* 1980).

An important aspect of the results of these laboratory

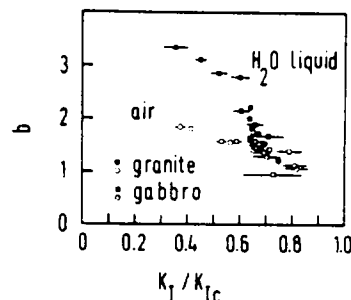


Fig. 8. Influence of stress intensity factor (normalized with respect to  $K_{Ic}$ ) on the  $b$ -value (the amplitude distribution parameter) for Westerley granite and Black gabbro in air of 30% r.h. and in liquid water. Horizontal bars denote the stress range of these data.

acoustic emission studies lies in their potential application as a means of monitoring stress corrosion in the earth. Acoustic emissions with frequencies in the range 0.5–5 kHz have been detected with deeply buried geophones in seismically active areas (Teng & Henyey 1981). See also Weeks *et al.* (1978). Propagating fractures in petroleum reservoir rocks have also been monitored with arrays of acoustic emission transducers (Shuck & Keech 1977). Because these emissions occur on a time scale measured in seconds or minutes, rather than the much longer time scale associated with low frequency seismic events, a large enough number of events can be recorded in a reasonable time so as to establish statistically meaningful changes in amplitude and frequency distributions and seismicity rates.

### SOME GEOPHYSICAL APPLICATIONS OF SUBCRITICAL CRACK GROWTH

#### *Prediction of time- and rate-dependent failure and friction properties of rocks*

In principle, integration of the area under a crack velocity/stress intensity factor diagram can provide all the information needed to predict the time- and rate-dependent fracture strength of rocks. In practice, the problem is made more difficult by complex stress states and mixed mode crack growth problems and some simplifying assumptions are necessary.

For the simplest case of pure mode I fracture propagation the influence of stress rate on fracture stress ( $\sigma_f$ ) can be approximated by (Evans & Johnson 1975)

$$\sigma_f = [2\dot{\sigma}(n_1 + 1)/A_1 Y^{n_1} (n_1 - 2)^{a_1(n_1 - 2)}]^{1/(n_1 + 1)} \quad (15)$$

where  $a_1$  is the initial flaw size,  $\dot{\sigma}$  is the stress rate,  $Y$  is a geometrical constant and  $A_1$ ,  $n_1$  are constants in the equation  $v = A_1 K_{I1}^{n_1}$  describing the region 1 stress corrosion behaviour of the material. Atkinson (1980) has used this equation successfully to predict the influence of stress (strain) rate on the tensile fracture stress of Arkansas novaculite in water at 20°C. It was found that at a strain rate faster than  $\sim 6 \times 10^{-5} \text{ s}^{-1}$  stress corrosion does not appreciably influence the tensile fracture stress, but at lower strain rates there is a monotonic reduction in strength from a maximum value of  $72 \text{ MN m}^{-2}$  in the absence of stress corrosion effects to approximately  $40 \text{ MN m}^{-2}$  at a strain rate of  $10^{-10} \text{ s}^{-1}$ .

The time-to-failure ( $t_f$ ) at a constant tensile stress ( $\sigma$ ) is also given by a similar integration of the  $K_{I1}$ - $v$  diagram (Evans 1972). It is found that

$$t_f = 2/\sigma^2 Y^2 \int_{K_{I1}}^{K_{Ii}} (K_{I1}/v) dK_{I1} \quad (16)$$

where  $K_{Ii}$  is the stress intensity factor associated with the initial flaw size.

Henry & Paquet (1976) have used equations based on

(15) and (16) to predict the influence of tensile stress on time-to-failure and strain rate on tensile fracture stress of calcite rocks.

Das & Scholz (in press) have developed a simple theoretical approach to predicting the time-to-failure of an earthquake rupture subject to stress corrosion. Provided that the static stress drop is independent of time, then time-to-failure is given by

$$t_f = (X_0/v_0)(2/n_1 - 2) \quad (17)$$

where  $X_0$  is the earthquake rupture radius and  $v_0$  the rupture velocity at the threshold stress intensity, and  $n_1$  is the stress corrosion index for region 1 behaviour. Note that here the time-to-failure depends only on the initial conditions and  $n_1$  and not on the final conditions as in the analysis of Evans (1972).

Mizutani *et al.* (1977) and Soga *et al.* (1979) have developed an equation that is a reasonably good predictor of the ultimate compressive strength of basalt, granite and quartz as a function of strain rate, humidity and temperature. They assumed that brittle failure in rocks occurs by the interaction of numerous small cracks that form parallel to the loading axis under the influence of the applied stress and the moisture content at crack tips. If the stress is applied at a slow rate and moisture is abundant at crack tips then the cracks will grow to be large and coalesce into a failure plane at low stress. If the stress is applied rapidly and the moisture content is low then the existing cracks will not relieve the stress concentrations and many new small cracks are formed. In the latter case failure occurs by the coalescence of a larger number of smaller cracks. Assuming that for a given crack configuration (size, shape and distribution) the rock will fail at a stress ( $\sigma_u$ ) when the cracks have reached an average critical length and that the crack growth is governed by an activated mechanism (stress corrosion by water), then

$$\sigma_u = D \{ (\ln \dot{\sigma} - \ln T - n \ln p_{\text{H}_2\text{O}} - B) RT + U \} \quad (18)$$

where  $\dot{\sigma}$  = applied stress rate,  $p_{\text{H}_2\text{O}}$  is the partial pressure of water,  $n$  = the order of the chemical reaction in stress corrosion (1 in this case),  $R$  and  $T$  are the gas constant and the absolute temperature, respectively,  $U$  is the activation energy for stress corrosion and  $D$  and  $B$  are constants that depend on activation volume, initial crack configuration and rock type.

Theories of stress corrosion have also been used by Scholz (1968) and by Cruden (1970) to develop theories of compressive creep in brittle rocks.

Anderson & Tiernan (1980) have produced a simple stress corrosion model of aseismic creep in fault zones which is envisaged as a slow breaking and reforming of asperities which are in contact along a fault plane. Thus macroscopic creep deformation measured at the surface actually consists of relatively slow rupturing on a microscopic scale.

The creep rate measured at the surface ( $\dot{\epsilon}_{\text{creep}}$ ) is given by the time required for cracks to grow a length,  $\delta$ , through asperities ( $\delta$  being a characteristic distance for asperity disruption) and cause them to transfer their loads to neighbouring asperities which are on the average,

separated by a distance  $\bar{R}$ . The creep rate is crudely given by

$$\dot{\epsilon}_{\text{creep}} = v \left( \frac{1}{\epsilon} \cdot \frac{\delta}{\bar{R}} \right) \quad (19)$$

where  $v$  is the microscopic crack growth velocity,  $\epsilon$  is the strain resulting from stress relaxation in the fault zone and  $\delta/\bar{R}$  may reasonably be expected to vary between 1.0 and 0.1.

#### Modelling earthquake rupture

There have been numerous suggestions that stress corrosion may play an important role in various time-dependent earthquake phenomena (Scholz 1972, Martin 1972, Bonafede *et al.* 1976, Atkinson 1979, 1980, Rice 1979, Rudnicki 1980). Recently, however, Das & Scholz (1981) have taken these speculations an important stage further and developed a simple, yet extremely comprehensive theory of shallow earthquake rupture based upon stress corrosion crack growth of a two-dimensional circular crack. This theory manages to predict virtually the whole gamut of observed earthquake phenomena (slow earthquakes, multiple events, delayed multiple events, postseismic rupture growth and afterslip, foreshocks and aftershocks). The theory also predicts that there must be a nucleation stage prior to an earthquake and predicts its form.

Das & Scholz (1981) obtain their results by combining two simple, but fundamental concepts. Firstly, from fracture mechanics

$$K = C\Delta\tau\sqrt{x} \quad (20)$$

and secondly, from stress corrosion theory

$$K = K_0 \left( \frac{\dot{X}}{v_0} \right)^{1/n} \quad (21)$$

where  $K$  is the stress intensity factor,  $\Delta\tau$  is the stress drop,  $X$  is the rupture length and  $\dot{X}$  the rupture velocity,  $C$  is a geometrical factor and  $K_0$ ,  $v_0$ ,  $n$  are material constants.  $K_0$  and  $n$  are the stress corrosion limit and stress corrosion index respectively.

A very important insight that is incorporated into Das & Scholz's model is that a major fault is not an homogeneous surface; a point that has been strongly emphasized in the past by geologists. The applied stress, and hence  $K$ , and the material properties  $K_0$  and  $n$  will be functions of position on the fault plane. To avoid the complexities of considering earthquake rupture as a stochastic growth process Das & Scholz consider only gross inhomogeneities, termed barriers (after Das & Aki 1977).

Tectonic stress is believed to increase in the earth's crust at a very slow rate and it is released when an earthquake occurs. This is equivalent to an increase in  $K$  until  $K_c$  is reached and the earthquake initiates. Stress corrosion theory, however, suggests a fracture criterion that is incompatible with this simplistic model. It predicts that propagation of the earthquake fault begins when  $K = K_0$

and it quasistatically accelerates as  $K$  approaches  $K_c$ . Thus, on this model an earthquake must be preceded by some precursory slip.

The size of a nucleation zone and the time scale of the process depend only upon  $n$  and  $K_0$  and their spatial distribution on the fault surface. Das & Scholz estimate the time from which the crack starts growing subcritically to that when it reaches instability, the nucleation time ( $t_f$ ) from equation (17). Estimates of the time-to-failure, velocity and rupture size immediately (1 second) before failure for physically reasonable values of  $X_0$ , and  $v_0$  and  $n$  from Atkinson (1979) leads to the conclusion that the majority of rupture growth occurs in the last few hours before an earthquake. This may explain why precursory slip on earthquake faults is not more commonly observed. An example of earthquake rupture growth by stress corrosion is shown in Fig. 9.

Some limitations to the Das & Scholz theory are as follows. Firstly, it assumes that stress corrosion influences crack growth in modes II and III. Although stress corrosion has only been observed in crack growth in mode I there is no obvious reason why mode II and III should not show the same phenomenon. Secondly, the simple form of the  $K_1-v$  curve on which Das & Scholz base their predictions could be due to mechanisms other than stress corrosion, although this would not materially alter their results. Thirdly, their analysis assumes only one large crack and their somewhat pessimistic view of earthquake precursors is based on that. In nature many smaller cracks might be involved in subcritical growth and the subsequent strain change might be sufficiently large to be measurable at the surface. Furthermore, quasistatic growth of numerous smaller ruptures or microscopic grain size level cracks may lead to the development of other precursory phenomena of sufficiently large magnitude that they can be observed. Finally, under conditions where free water is absent and stress corrosion is presumably impossible, earthquake patterns will not be predictable on the basis of the above model. This is presumably the case with many deep focus earthquakes which only rarely are accompanied by aftershocks.

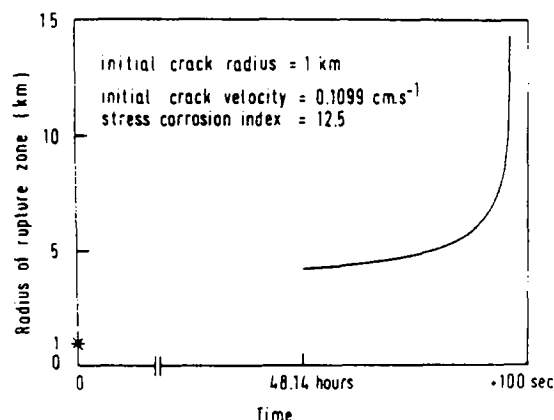


Fig. 9. An example of the likely trend in the growth of an earthquake rupture controlled by stress corrosion. After Das & Scholz (1981). Note discontinuous and non-uniform time scale. Star denotes initial radius of rupture. Other relevant conditions are given on the figure.

One of the advantages of invoking stress corrosion crack growth as a necessary precondition for rupture in the earth's crust is that the difference between so-called 'aseismic' and seismic fault zones also becomes clear. The difference between seismic and aseismic fault segments is merely a difference in spatial-temporal variation in material properties and environment along fault zones. Moreover, the difference between 'slow' and 'normal' earthquakes, multiple event earthquakes, delayed multiple event earthquakes and aftershocks is also largely one of scale.

#### *Stability of hydrofractures*

The extraction of thermal energy from hot, initially dry rocks at depths in the earth's crust involves in theory the creation of a large quasi-vertical crack in these rocks by hydrofracturing. To extract heat from the rock, cold water is circulated within the crack while it is held open by pressurizing the water to exceed the local horizontal stress.

The cold water is heated by contact with the large surface area of rock and is then pumped to the surface for use (e.g. LASL project in New Mexico, Cornish project).

For a given size of hydrofracture the volume of the crack will increase linearly with the differential pressure which is given by

$$\Delta P = P_{\text{fluid}} - \sigma_3 \quad (22)$$

where  $P_{\text{fluid}}$  is the fluid pressure in the hydrofracture and  $\sigma_3$  is the horizontal stress in the rock, assuming the crack to be vertical. The volume of the crack and hence the flow of water and energy yield are limited by the maximum fluid pressure which the crack can sustain without growing appreciably during the proposed lifetime of the well (Demarest 1976). If the proposed life of the well is measured in tens of years then an appreciable amount of crack growth would be hundreds of metres (based upon LASL experiments). Thus, to avoid seriously degrading the energy yield of the geothermal reservoir  $\Delta P$  must not be greater than a value that leads to stress corrosion crack growth of  $c. 10 \text{ m y}^{-1}$  ( $\approx 3 \times 10^{-7} \text{ m s}^{-1}$ ).

Stress corrosion data for Westerley granite (Atkinson & Rawlings 1981) can be used as a model of likely behaviour of reservoir rocks so that the value of  $K_I$  required to produce a crack velocity of  $10^{-7} \text{ m s}^{-1}$  can be estimated. This is approximately  $1.1 \text{ MN m}^{-3/2}$  for liquid water at  $20^\circ\text{C}$ .  $K_I$  is related to  $\Delta P$  through

$$K_I = \Delta P(2/\pi)^{1/2}(a)^{1/2} \quad (23)$$

where  $a$  is the radius of the circular crack.

The working down-hole environment of a dry granite geothermal well, such as that developed by Los Alamos Scientific Laboratories, involves pressurized water at a temperature of  $c. 200^\circ\text{C}$  and depths of 2–5 km. An increase in temperature of  $200^\circ\text{C}$  should increase the rate of crack propagation in granite by about one order of magnitude (Atkinson 1979, 1980), but the increased water pressure at these depths will probably inhibit stress corrosion. A crack velocity of  $10^{-7} \text{ m s}^{-1}$  might be

expected to develop, therefore, under a stress intensity of  $c. 1 \text{ MN m}^{-3/2}$ .

Taking  $K_I$  for fast hydrofracturing equal to  $K_{Ic}$  leads to the conclusion that  $K_I$  in the well should not exceed approximately 0.6 of the  $K_I$  for initial hydrofracturing otherwise extraction of energy from the hot, initially dry rocks could be seriously degraded.

A similar hydrofracturing technique is used in stimulating 'tight' oil and gas reservoirs. Clearly, great care should be taken to ensure that hydrofractures so created do not propagate subcritically into zones of high fluid conductivity (e.g. faults, permeable strata) and thereby breach the integrity of the reservoir.

Because of the potential for subcritical propagation of hydrofractures during slow tectonic rates of loading, stress estimates based upon fast fracture analyses of mineralized extension cracks developed (i) in rocks deformed by Ramsay's 'crack-seal' mechanism of rock deformation (Ramsay 1980), or (ii) in, low stress dilatancy around fault zones (Sibson 1981) are likely to be upper limits.

#### *Fracture mechanics of lunar rocks*

The nonhydrostatic shape of the moon, the remarkably deep moonquakes and the existence of mascons strongly suggest that the lunar interior has both a high strength and a high viscosity (see Mizutani *et al.* 1977). How can one reconcile the apparently high strength of the lunar lithosphere sustained for periods of  $10^9$  years with the inference that temperatures may have been abnormally high by terrestrial standards (Anderson & Hanks 1972, Duba *et al.* 1976)?

The lunar lithosphere and surface are at high vacuum, and free water is thought to be generally absent so that stress corrosion is unlikely to occur (Martin 1972, Mizutani *et al.* 1977). The apparently high strength of the lunar lithosphere can thus simply be explained. See also the experimental results of Mizutani *et al.* (1977) and Soga *et al.* (1979) on analogues of lunar glasses and rock which tend to confirm this hypothesis.

#### *Magmatic intrusions*

Anderson & Grew (1977) and Runcorn (1980) have pointed out that there are several weaknesses in the so-called 'hot-spot' theory that attempts to explain the alignment of intra-plate volcanic islands (e.g. Hawaiian chain) by proposing that stationary plumes of volcanic activity are overridden by the lithospheric plates. Apart from the results of considering the balance between viscous and inertial forces (Runcorn 1980), the most obvious objection is that the direction and rate of plate movements deduced from the assumption of fixed 'hot spots' are inconsistent with plate motions deduced by other means (Jackson 1976). This has led to the proposition that the 'hot spots' are not fixed but migrate.

A simpler and more elegant proposition due to Anderson & Grew (1977) and others is that the linearity of these

volcanic chains is related to the growth of a slowly propagating crack in the plate under the influence of stress corrosion. The rate of propagation of volcanic chains can attain velocities of  $1\text{--}30\text{ cm y}^{-1}$  (Jackson 1976, Anguita & Hernan 1975) which are consistent with observed rates of stress corrosion in rocks. The apparent rate of fracture propagation in the Anderson/Grew model is controlled by the bending moment in the plate and only indirectly by the plate velocity. Thus, as is observed, the direction and rate of plate movements can be different from the propagation of volcanic chains. The non linear rates of propagation in some chains can be explained by noting that even for a continuous crack, volcanoes will be rare except in those few places where all the conditions for magma intrusion and surface eruption are satisfied. Magmas might rise repeatedly through older weakened, previously cracked, portions of the lithosphere or at the advancing portion of the crack front (Vogt 1974).

A factor determining the rate of fracture propagation may be the highly acidic fluids and volatiles that precede magmatic intrusions. However, under the high pressures and temperatures ( $600^\circ\text{C}$  and above) likely to obtain near cracks into which magma and volatiles intrude it is highly likely that plastic flow at crack tips will occur. This will blunt the cracks and thus to maintain the same rate of stress-corrosion crack growth the stress would need to be raised. At these higher stresses crack growth may occur more rapidly by a process involving heterogeneous plastic flow rather than stress corrosion (Fig. 1).

#### *Relaxation of internal stresses in rock*

It is a relatively common observation that strains as large as  $10^{-3}$  occur in silicate rocks that are removed from quarries or drill holes or that are disturbed by sawing, drilling or loading. The spectacular experiments of Price (1966) are a good example of this phenomenon. Using experimental data as input Bruner (1980b) has made computer simulations of unloading rocks that suggest the most likely mechanism for the observed strain relaxation is stress corrosion.

## CONCLUSIONS

I have outlined some of the complexities of subcritical tensile failure in materials and presented a large body of experimental evidence to show that the subcritical growth of pre-existing cracks in rocks by stress corrosion is a common phenomenon under laboratory conditions. With few exceptions, however, the range of conditions explored in the laboratory represents only extremely shallow depths in the earth's crust. The extent to which stress corrosion is an important mechanism of tectonic deformation must still remain an open question. Nevertheless, a wide range of geophysical phenomena can plausibly be explained by invoking stress corrosion crack growth, and some important examples are given. Under appropriate environmental conditions, some form of subcritical crack

growth other than stress corrosion may occur which has approximately the same stress intensity factor–crack velocity relationship. This area has yet to be explored. Data on the influence of pressure on stress corrosion are urgently needed.

Unfortunately, the physical interpretation of crack propagation and static fatigue theories is hampered because with the sort of data that is readily available an unequivocal distinction between different theories cannot be reached. As Wiederhorn (1978) has pointed out, the same set of data is often used to justify fracture theories that have very different starting assumptions and physical bases.

Two factors cause most of the problems; the stress dependence of crack growth rate and the activation enthalpy for crack propagation. Because in a static fatigue test on rock, one order of magnitude change in stress can only be covered by between 20 and 35 orders of magnitude in time, a variety of theories will adequately fit the same data. The activation enthalpies for crack propagation are generally rather low (c.  $50\text{--}100\text{ kJ mole}^{-1}$ ). Not only are these low values of activation enthalpy intrinsically hard to measure (Swanson 1980), but their determination by an empirical fit of experimental data depends on the form of the equation chosen for the fit, and hence on the physical model of crack propagation adopted. Furthermore, the activation enthalpies for competing deformation mechanisms are often rather similar (e.g. for quartz, Atkinson 1979).

Finally, this article has concentrated to a large extent on mode I crack propagation. This was inevitable as no data were available for rock on subcritical crack propagation in other modes. It was implicit, however, in much of the discussion on applications of stress corrosion theory that this mechanism does occur in modes II and III (shear modes). Moreover, it was assumed that the form of equations describing stress corrosion in mode II and III should be the same as that for mode I crack propagation, even if the values of parameters in these equations differed. These assumptions urgently need experimental verification under simulated crustal conditions.

*Acknowledgements*—Financial support for much of the work reported here was provided by the U.S. Geological Survey in the form of contract numbers 14-08-0001-17662 and 14-08-0001-18325. This study forms part of the U.S. National Earthquake Hazards Reduction Program. Additional funds were provided by the British Natural Environment Research Council under grant GR3/3716.

The assistance of Paul Dennis and Philip Meredith in the preparation of this paper is gratefully acknowledged. Some of the experimental work described here was undertaken with facilities provided by Paul Ewing and Rees Rawlings of Imperial College. Michael Ashby of Cambridge University has continued to influence strongly my view of the mechanics of materials. I wish to thank him for the provision of numerous reprints of his work.

## REFERENCES

- Anderson, D. L. & Hanks, T. C. 1972. Is the moon hot or cold? *Science* N.Y. **178**, 1245–1249.  
Anderson, O. L. & Grew, P. C. 1977. Stress corrosion theory of crack

- propagation with application to geophysics. *Rev. Geophys. Space Phys.* **15**, 77–104.
- Anderson, O. L. & Tiernan, M. F. 1980. Stress corrosion cracking in premonitory earthquake events. Final technical report to managers of US National Earthquake Hazards Reduction Program, Contract No: 14-08-0001-16798.
- Anguita, F. & Hernan, F. 1975. A propagating fracture model versus a hot spot origin for the Canary Islands. *Earth Planet. Sci. Lett.* **27**, 11–19.
- Ashby, M. F., Gandhi, C. & Taplin, D. M. R. 1979. Fracture-mechanism maps and their construction for F.C.C. metals and alloys. *Acta Metall.* **27**, 699–729.
- Atkinson, B. K. 1979. A fracture mechanics study of subcritical tensile cracking of quartz in wet environments. *Pure appl. Geophys.* **117**, 1011–1024.
- Atkinson, B. K. 1980. Stress corrosion and the rate-dependent tensile failure of a fine-grained quartz rock. *Tectonophysics* **65**, 281–290.
- Atkinson, B. K. & Meredith, P. G. 1981. Stress corrosion cracking of quartz: A note on the influence of chemical environment. *Tectonophysics* **77**, T1–T11.
- Atkinson, B. K. & Rawlings, R. D. 1979. Acoustic emission during subcritical and fast tensile cracking of Westerley granite and a gabbro. *EOS. Trans. Am. geophys. Un.* **60**, 740.
- Atkinson, B. K. & Rawlings, R. D. 1981. Acoustic emission during stress corrosion cracking in rocks. In: *Earthquake Prediction*. Fourth Maurice Ewing Symposium, New York, A.G.U., 605–616.
- Atkinson, B. K., Price, N. J., Dennis, S. M., Meredith, P. G. & Holloway, R. F. 1980. Mechanisms of fracture and friction of crustal rock in simulated geologic environments. Semi-annual technical report to managers of U.S. National Earthquake Hazards Reduction Program, Contract No.: 14-08-0001-18325.
- Bonafede, M., Fazio, D., Mulargia, F. & Boschi, E. 1976. Stress corrosion theory of crack propagation applied to the earthquake mechanism. A possible basis to explain the occurrence of two or more large seismic shocks in a geologically short time interval. *Boll. Geofis. teor. appl.* **19**, 377–403.
- Brown, S. D. 1979. Multibarrier kinematics of brittle fracture: I. Stress dependence of the subcritical crack velocity. *J. Am. Ceram. Soc.* **62**, 515–524.
- Bruner, W. M. 1980a. Effects of time-dependent crack growth on the unroofing and unloading behaviour of rock. Unpublished Ph.D. thesis, University of California, Los Angeles.
- Bruner, W. M. 1980b. Relaxation of internal stresses in rocks by time-dependent crack growth. *EOS. Trans. Am. geophys. Un.* **61**, 372.
- Byerlee, J. D. & Peselnick, L. 1970. Elastic shocks and earthquakes. *Naturwissenschaften* **57**, 82–85.
- Charles, R. J. 1958. Dynamic fatigue of glass. *J. appl. Phys.* **29**, 1657–1662.
- Charles, R. J. & Hillig, W. B. 1962. Kinetics of glass failure of stress corrosion. In: *Symposium sur la Résistance Mécanique du Verre et les Moyens de l'Améliorer*. Union Scientifique Continentale du Verre, Charleroi, Belgium, 511–527.
- Cruden, D. M. 1970. A theory of brittle creep in rock under uniaxial compression. *J. geophys. Res.* **75**, 3431–3442.
- Das, S. & Aki, K. 1977. Fault plane with barriers: A versatile earthquake model. *J. geophys. Res.* **82**, 5658–5670.
- Das, S. & Scholz, C. H. 1981. Theory of time-dependent rupture in the earth. *J. geophys. Res.* **86**, 6039–6051.
- Dehart, R. C. & Liebowitz, H. 1968. The influence of ambient pressure on the stress corrosion susceptibility of metals. *Engng Fract. Mech.* **1**, 129–135.
- Demarest, H. H. Jr. 1976. Application of stress corrosion to geothermal reservoirs. Informal Report LA-6148-ms, Los Alamos Scientific Laboratory.
- Dennis, P. F. & Atkinson, B. K. 1982. Point defect chemistry, diffusion and deformation mechanism maps for quartz. *Earth Planet. Sci. Lett.* Submitted for publication.
- Duba, A., Heard, H. C. & Schock, R. N. 1976. Electrical conductivity of orthopyroxene to 1400°C and the resulting selenotheny. *Proc. 7th Lunar Sci. Conf.* 3173–3181.
- Dunning, J. D., Lewis, W. L. & Dunn, D. E. 1981. Chemomechanical weakening in the presence of surfactants. *J. geophys. Res.* **85**, 5344–5354.
- Evans, A. G. 1972. A method for evaluating the time-dependent failure characteristics of brittle materials — and its application to polycrystalline alumina. *J. Mater. Sci.* **7**, 1137–1146.
- Evans, A. G. & Graham, L. J. 1975. A model for crack propagation in polycrystalline ceramics. *Acta metall.* **23**, 1303–1312.
- Evans, A. G. & Johnson, H. 1975. The fracture stress and its dependence on slow crack growth. *J. Mater. Sci.* **10**, 214, 222.
- Evans, A. G. & Linzer, M. 1973. Failure prediction in structural ceramics using acoustic emission. *J. Am. Ceram. Soc.* **56**, 575–581.
- Fuller, E. R., Jr. & Thomson, R. 1980. Theory of chemically assisted fracture. Part 2. Atomic models of crack growth. *J. Mater. Sci.* **15**, 1027–1034.
- Gandhi, C. & Ashby, M. F. 1979. Fracture mechanism maps for materials which cleave: F.C.C., B.C.C. and H.C.P. metals and ceramics. *Acta metall.* **27**, 1565–1602.
- Gerberich, W. W. 1974. On the pressure dependence of threshold stress intensity. *Engng Fract. Mech.* **6**, 405–407.
- Granryd, L. A., Sondergeld, C. H. & Estey, L. H. 1980. Precursory changes in acoustic emissions prior to the uniaxial failure of rock. *EOS. Trans. Am. geophys. Un.* **61**, 372.
- Hartley, N. E. W. & Wilshaw, T. R. 1973. Deformation and fracture of synthetic  $\alpha$ -quartz. *J. Mater. Sci.* **8**, 265–278.
- Henry, J. P. 1978. Mécanique lineaire de la rupture appliquée à l'étude de la fissuration et de la fracture de roches calcaires. Unpublished Ph.D. thesis, Université des Sciences et Techniques de Lille.
- Henry, J. P. & Paquet, J. 1976. Mécanique de la rupture de roches calcitiques. *Bull. Soc. geol. Fr.* **7 Ser.** **18**, 1573–1582.
- Irwin, G. R. 1958. Fracture. In: *Handbuch der Physik* **6**, (edited by Flüge, S.) Springer, Berlin, 551–590.
- Jackson, E. D. 1976. Linear volcanic chains on the Pacific plate. In: *The Geophysics of the Pacific Ocean Basin and its Margin*. *Geophys. Monogr. Ser.* **19** (edited by Woolard, G. P., Sutton, G. H., Manghnani, M. H. & Moberly, R.) American Geophysical Union, Washington, D.C. 319–335.
- Kranz, R. L. 1980. The effects of confining pressure and stress difference on static fatigue of granite. *J. geophys. Res.* **85**, 1854–1866.
- Krausz, A. S. 1978. The deformation and fracture kinetics of stress corrosion cracking. *Int. J. Fract.* **14**, 5–15.
- Lawn, B. R. 1975. An atomistic model of kinetic crack growth in brittle solids. *J. Mater. Sci.* **10**, 469–480.
- Lawn, B. R. & Wilshaw, T. R. 1975. *Fracture of Brittle Solids*, Cambridge Univ. Press, Cambridge, 204 pp.
- Marsh, D. M. 1964. Plastic flow in glass. *Proc. R. Soc.* **A279**, 420–435.
- Martin, R. J. III, 1972. Time-dependent crack growth in quartz and its application to the creep of rocks. *J. geophys. Res.* **77**, 1405–1419.
- Martin, R. J. III & Durham, W. B. 1975. Mechanisms of crack growth in quartz. *J. geophys. Res.* **80**, 4837–4844.
- Meredith, P. G. & Atkinson, B. K. 1981. Acoustic response during stress corrosion of Whin Sill dolerite. *Geophys. J. R. astr. Soc.* **65**, 278.
- Mizutani, H., Spetzler, H., Getting, I., Martin, R. J. III & Soga, N. 1977. The effect of outgassing upon the closure of cracks and the strength of lunar analogues. *Proc. 8th Lunar Sci. Conf.*, 1235–1248.
- Norton, M. G. & Atkinson, B. K. 1981. Stress-dependent morphological features on fracture surfaces of quartz and glass. *Tectonophysics* **77**, 283–295.
- Peck, L. 1980. Stress corrosion cracking of quartzite. *EOS. Trans. Am. geophys. Un.* **61**, 361.
- Price, N. J. 1966. *Fault and Joint Development in Brittle and Semi-Brittle Rock*. Pergamon, Oxford.
- Ramsay, J. G. 1980. The crack-seal mechanism of rock deformation. *Nature. Lond.* **284**, 135–139.
- Rice, J. R. 1979. Theory of precursory processes in the inception of earthquake rupture. *Beitr. Geophys.* **88**, 91–127.
- Rudnicki, J. W. 1980. Fracture mechanics applied to the earth's crust. *A. Rev. Earth Planet. Sci.* (edited by Donath, F. A. et al.) *Annual Reviews Inc.* **8**, 489–525.
- Runcorn, S. K. 1980. Some comments on the mechanism of continental drift. *Mechanisms of Continental Drift and Plate Tectonics* (edited by Davies, P. A. & Runcorn, S. K.) Academic Press, London, 193–198.
- Sano, O. & Ogino, S. 1980. Acoustic emission during slow crack growth. *Tech. Rep. Yamaguchi Univ.* **2**, 381–388.
- Schmidt, R. A. 1976. Fracture mechanics of oil shale — unconfined fracture toughness, stress corrosion cracking and tension test results. *Proc. 18th U.S. Symposium Rock Mechanics*. Keystone, Colorado, 2A2-1–2A2-6.
- Scholz, C. H. 1968. Mechanism of creep in brittle rock. *J. geophys. Res.* **73**, 3295–3302.
- Scholz, C. H. 1972. Static fatigue of quartz. *J. geophys. Res.* **77**, 2104–2114.
- Schwartz, M. W. & Mukherjee, A. K. 1974. The migration of point defects in crack tip stress fields. *Mat. Sci. Engng* **13**, 175–179.
- Shuck, L. Z. & Keech, T. W. 1977. Monitoring acoustic emission from propagating fractures in petroleum reservoir rocks. In: *Proc. First Conference on Acoustic Emission/Microseismic Activity in Geological Structures and Materials* (edited by Hardy, H. R. Jr. & Leighton, F. W.) Trans. Tech. Publications, Clausthal, Germany, 309–338.
- Sibson, R. H. 1981. Low stress hydrofracture dilatancy: controls on its

- development in thrust, wrench and normal fault terrains. *Nature Lond.* **289**, 665-667.
- Soderberg, R. 1972. On the growth of intercrystalline wedge-cracks during creep-deformation. *J. Mater. Sci.* **7**, 1373-1378.
- Soga, N., Spetzler, H. & Mizutani, H. in press. Comparison of single crack propagation in lunar analogue glass and the failure strength of rocks. *Proc. 10th Lunar Sci. Conf.*
- Stevens, R. N. & Dutton, R. 1971. The propagation of Griffith cracks at high temperatures by mass transport processes. *Mat. Sci. Engng* **8**, 220-234.
- Swain, M. V., Williams, J. S., Lawn, B. R. & Beek, J. J. H. 1973. A comparative study of the fracture of various silica modifications using the Hertzian test. *J. Mater. Sci.* **8**, 1153-1164.
- Swanson, P. L. 1980. Stress corrosion cracking in Westerley granite. Unpublished M.Sc. thesis, Colorado University.
- Teng, T. & Henyey, T. L. in press. Acoustic emission as a possible earthquake precursor. *Proc. Third Ewing Symposium on Earthquake Prediction* AGU, Washington, D.C.
- Thomson, R. 1980. Theory of chemically assisted fracture. Part 1. General reaction rate theory and thermodynamics. *J. Mat. Sci.* **15**, 1014-1026.
- Vogt, P. R. 1974. Volcano spacing, fractures, and thickness of the lithosphere. *Earth Planet. Sci. Lett.* **21**, 235-252.
- Waza, T., Kurita, K. & Mizutani, H. 1980. The effect of water on the subcritical crack growth in silicate rocks. *Tectonophysics* **67**, 25-34.
- Weeks, J. D., Lockner, D. & Byerlee, J. 1978. Change in b-values during movement on cut surfaces in granite. *Bull. seism. Soc. Am.* **68**, 333-341.
- Wiederhorn, S. M. 1968. Moisture-assisted crack growth in ceramics. *Int. J. Fract. Mech.* **4**, 171-177.
- Wiederhorn, S. M. 1974. Subcritical crack growth in ceramics. In: *Fracture Mechanics of Ceramics*, vol. 2 (edited by Bradt, R. C., Hasselman, D. P. H. & Lange, F. F.) Plenum Press, New York, 613-646.
- Wiederhorn, S. M. 1978. Mechanisms of subcritical crack growth in glass. In: *Fracture Mechanics of Ceramics*, vol. 4 (edited by Bradt, R. C., Hasselman, D. P. H. & Lange, F. F.) Plenum Press, New York 549-580.
- Wiederhorn, S. M. & Bolz, L. H. 1970. Stress corrosion and static fatigue of glass. *J. Am. Ceram. Soc.* **53**, 543-548.
- Wiedmann, G. W. & Holloway, D. G. 1974. Plastic flow-slow crack propagation and static fatigue in glass. *Physics Chem. Glasses* **15**, 68-75.
- Wilkins, B. J. S. 1980. Slow crack growth and delayed failure of granite. *Int. J. Rock Mech. Min. Sci. Geomech. Abstr.* **17**, 365-369.
- Williams, J. G. & Marshall, G. P. 1975. Environmental crack and craze growth phenomena in polymers. *Proc. R. Soc.* **A342**, 55-77.